ELSEVIER

Nuclear Instruments and Methods in Physics Research A 452 (2000) 67–80

NUCLEAR INSTRUMENTS & METHODS IN PHYSICS RESEARCH Section A

www.elsevier.nl/locate/nima

# Cosmic-ray tests for quality control of the CDF plug upgrade EM calorimeter and the CDF plug preshower detector

T. Asakawa, K. Hara, K. Hata, T. Kadotani, H. Kawamoto, T. Kikuchi, S.H. Kim, K. Kondo, T. Kuwabara, M. Okura, H. Okutomi, M. Sano, Y. Seiya*, T. Shibayama, T. Suzuki, S. Takashima, K. Takikawa, M. Tanaka, Y. Tanaka, T. Uchida, T. Watanabe

*Institute of Physics, University of Tsukuba, Tsukuba, Ibaraki 305, Japan*

Received 23 December 1999; accepted 11 February 2000

**Abstract**

The CDF Plug Upgrade electromagnetic (EM) calorimeter and the preshower detector consist of tile-fiber elements forming a projective tower geometry. Each of the 23 longitudinal layers is separated into 24 units in the azimuthal direction. Cosmic-ray tests as a quality control of these mechanically basic units, called the 15° units, were carried out since January 1995 and completed in June 1996. All the units amounting to a total 1200 units were processed. By using HAMAMASU R4125 for the photon readout, the average light yields were measured to be 5.8 and 21 photoelectrons for the EM and the preshower units, respectively. The light yield variation along the longitudinal layers of EM tower was measured to be 10%. A GEANT-simulation study using the results of the cosmic-ray tests was performed for a realistic calorimeter configuration. It was found that the simulated energy resolution was consistent with the requirement of $\Delta E/E = \sqrt{(16\%)^2/E + (1\%)^2}$ ($E$ in GeV). Adding preshower response to EM response improved in particular the linearity of the calorimeter. It was possible to achieve the non-linearity of 1% level for energies in the range of 10–200 GeV. 

## 1. Introduction

The upgraded Tevatron collider at Fermilab will be operated in a 36-bunch mode with a bunch-crossing time of 396 ns, and eventually 108 bunches with 132 ns, in the forthcoming collider runs. In order to facilitate the best physics performance of the CDF detector in such a situation, the present electromagnetic (EM) gas calorimeters in the plug and the forward/backward regions will be replaced with a scintillator-based calorimeter [1,2].

The new plug EM calorimeter consists of sandwiches of absorber plates and scintilators with optical fiber readout. The absorber plate is made of lead 4.5 mm in thickness and stainless-steel sheets 0.5 mm in thickness on both sides of the lead plate. The scintillator plates are 4 mm thick. The number of longitudinal layers is 23 in which the first scintillator layer, the thickness of which increased to

* Correspondence address: Fermilab MS-318, P.O. Box 500, Batavia, IL 60510, USA. Tel.: +1-630-840-5670; fax: +1-630-840-2968.

*E-mail address:* seiya@fnal.gov (Y. Seiya).

0168-9002/00/$ - see front matter 
PII: S0168-9002(00)00352-1

10 mm is readout separately to serve as a preshower detector. The preshower detector is used for statistical separation of photons from neutral hadrons and also for the reduction of charged hadron background in electron identification. Each layer consists of 24 independent sub-assemblies called the 15° units in what follows. A 15° unit contains at most 20 scintillator segments so that the whole calorimeter system has a projective tower geometry. A scintillator segment is a complex of a scintillator plate (tile) and a wavelength-shifter (WLS) fiber for readout, and called the tile–fiber system. The tile–fiber systems are separated from each other by white paint which serves as a light shield and a reflector.

We use BICRON BC408 scintillator for the first layer and KURARAY SCSN38 scintillator for the rest of the layers. The WLS fiber is KURARAY Y11 with 0.83 mm diameter. The R&D results for the tile–fiber system are found in Refs. [3,4]. We use photomultiplier tubes (PMTs) as the photon readout. They are HAMAMATSU R4125 for the EM calorimeter and HAMAMATSU R5900-M16 for the preshower detector. The R5900-M16 is a multianode tube (MAPMT) with 16 channels.[1]

The upgraded calorimeter is expected to have a sampling fluctuation of 14%. The required energy resolution is $\Delta E/E = \sqrt{(16\%)^2/E + (1\%)^2}$, where $E$ is the energy in GeV, and the required non-linearity is 1% level for the energy range of 10–400 GeV [1,2]. By simulation studies, these requirements are translated to the following criteria for the optical quality of the EM 15° units (layer 2–23):

- the number of photoelectrons (pe) per minimum ionizing particle (MIP) is larger than 3;
- the light yield variation along the longitudinal layers of tower is smaller than 10%;
- the light leakage to adjacent tiles is smaller than 4%;
- the light yield variation along the tile surface (surface non-uniformity) is smaller than 2.5%.

[1] Each anode size is 4.0 mm × 4.0 mm. The quantum efficiency at the wavelength of 500 nm is $\simeq 10\%$ and the typical gain is $\simeq 10^7$ at $-900$ V.

For the preshower detector units (layer 1), we require 5 pe per MIP to ensure a good efficiency of detecting photon conversions. The light leakage for the preshower units is expected to be larger than that for the EM units because a thicker tile has a relatively larger geometrical acceptance for light from an adjacent tile. We require the light leakage to be smaller than 8% for the preshower units.

Under various quality controls at several production stages, the mass production of the 15° units was completed in February 1994 [5,6]. As a final quality control, cosmic-ray tests of all the 15° units were carried out from January 1995 to June 1996. In the quality requirements, the surface uniformity had been established by a quality control at an earlier production stage and it should not be affected in assembling the 15° units. Furthermore, its measurements by cosmic rays requires a long testing period because of a moderate event rate. The surface uniformity was, therefore, put outside of consideration in the quality control by cosmic rays.

This article summarizes cosmic-ray tests for the quality control of the total 1144 EM and 56 preshower 15° units including some spare units. The cosmic-ray test system is described in Section 2. The calculation of the light yield is explained in Section 3. The results of the cosmic-ray tests are given in Section 4. A simulation study of the calorimeter performance with the GEANT Monte Carlo program is described in Section 5. Conclusions are given in Section 6.

## 2. Cosmic-ray test system

Side views of the cosmic-ray test stand are shown in Fig. 1. The 15° units were put in a sliding tray. Two sets of plastic-scintillator hodoscopes were located over and under the tray. The outside of them was occupied by two sets of crossed module-arrays of drift chambers which provided tracking of cosmic rays with a position resolution of $\simeq 0.5$ mm. These chambers were the same type as developed by the Venus group for the TRISTAN experiment [7], but a modification was made by inserting delay chips on the anode-signal line to match with the timing delay of trigger signals. A hardener of iron with a thickness of 5 cm was

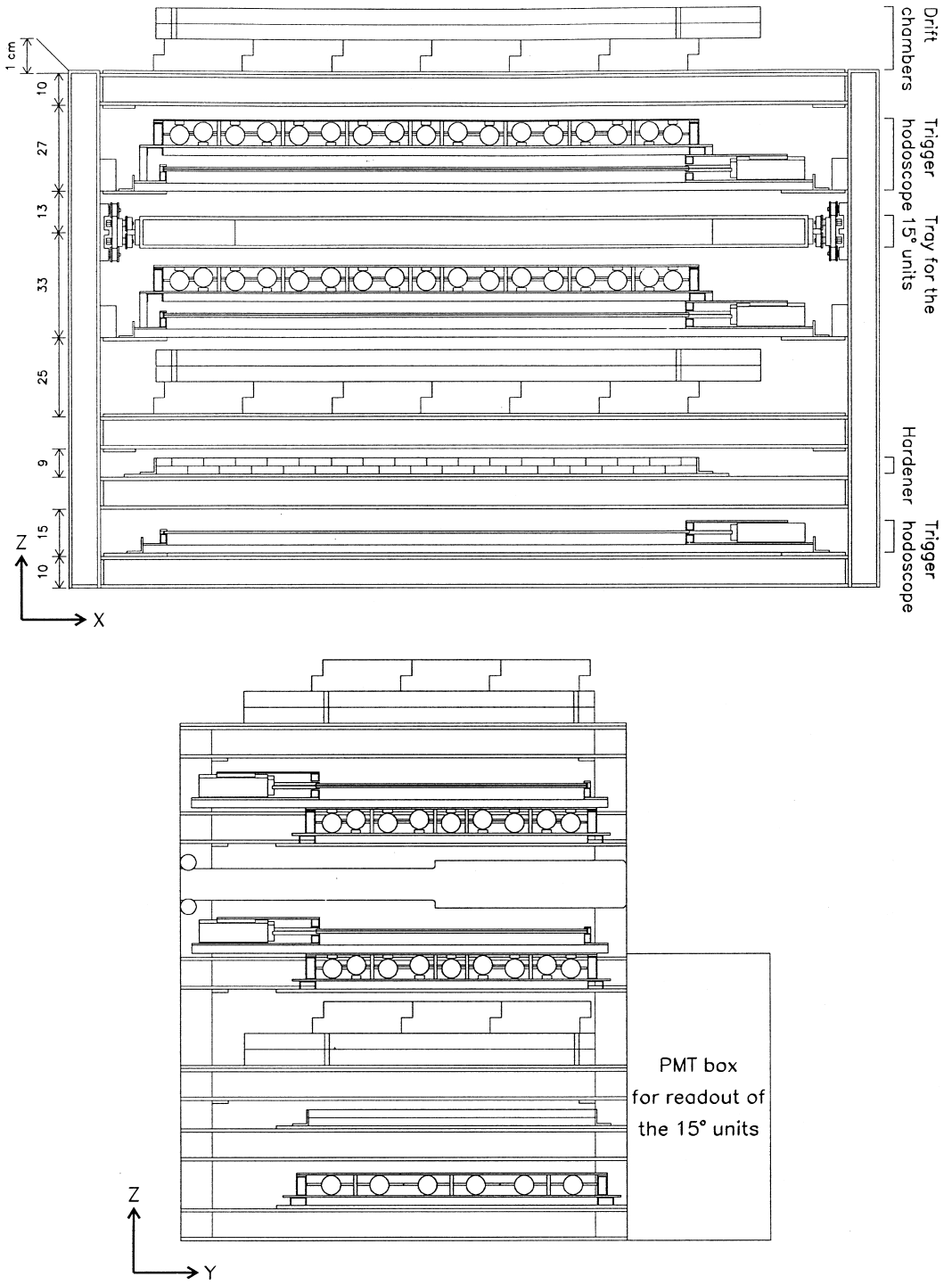


Fig. 1. Side views of the cosmic-ray test stand.

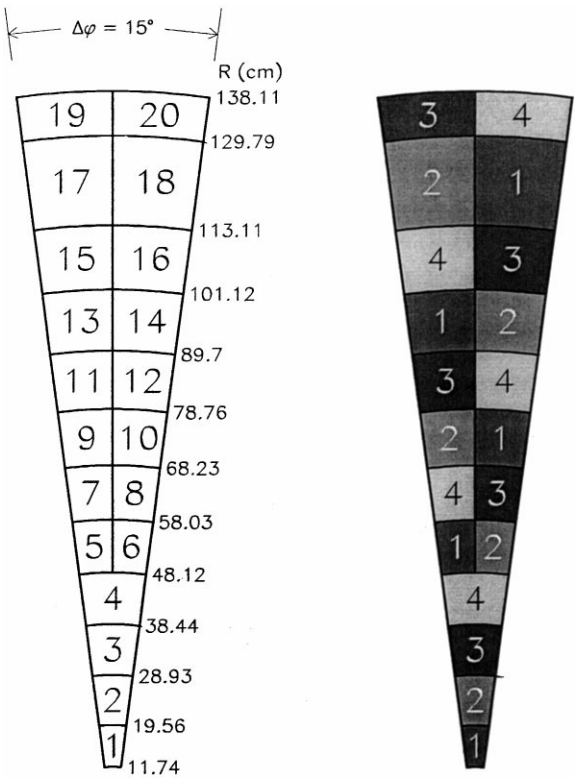


Fig. 2. Dimensions of the 15° unit of layer 12, the tile number assignment (left), and the phototube assignment to the tiles (right).

placed under the lower tracking system. It eliminated cosmic rays with momenta lower than 170 MeV/$c$. The bottom of the stand was a single plastic-scintillator array to signal cosmic rays penetrating the hardener. The coordinate system was defined as shown in the figure. The overall size of the stand was 255 cm long ($x$), 140 cm wide ($y$), and 183 cm high ($z$). The active area of the stand was 160 cm × 80 cm.

Typical dimensions of the 15° unit are shown in Fig. 2. A total 15 (9) EM (preshower) units arranged in three stacks of five (three) layers were processed in a single test. Four PMTs read one layer (three units). The tile number convention and the assignment of the four PMTs to the tiles are also shown in Fig. 2. This PMT assignment makes it possible to be sensitive to the light leakage to adjacent tiles. The same assignment was applied to other four layers using different sets of four PMTs, thus, a total of 20 PMTs were used. The readout PMTs were HAMAMATSU H1161GS which had the same photocathode (R4125) as the actual detector. They were operated at $-2000$ V. The PMTs and the 15° units were connected with readout clear-fibers as schematically shown in Fig. 3. The light from the 15° units was first transmitted to 10-fiber (0.9 mm diameter) cables of 3 m long at an optical connector (type A in Ref. [8]). The fiber cables were inserted through plastic tubes and entered a light-shielded box located at the back of the cosmic-ray test stand where the PMTs were housed (PMT box; see Fig. 1). Inside the PMT box, the 6-fiber cables were connected to a single distributor by another type of connector (type B [8]). The distributor was a complex of the total 80 clear fibers (1.0 mm diameter) of 1 m long, and it distributed input fibers to relevant PMTs according to the PMT-tile assignment.

We used the CAMAC system for data acquisition (DAQ). The DAQ machine was a DEC VAX3500 workstation. A trigger signal was five-fold coincidence of the scintillator counters, where hits were required to be at the same column and row of the upper and lower hodoscopes. This logic rejected tracks with large zenith angles, and the light yield variation due to the track angle variation was reduced to a comfortable level. CAMAC input-registers were used to store hit patterns of the hodoscopes and hit information from the drift chambers. Signals of the PMTs were digitized and stored by CAMAC ADCs which had a charge resolution of 0.25 pC/count. The DAQ efficiency was 85% and the trigger rate was $\simeq 20$ Hz.

## 3. Light yield measurement

We define the light yield as the number of photoelectrons ($N_{pe}$) and calculate it by $N_{pe} = (\mu - p)/(s - p)$, where $\mu$ is the average value of a pulse-height distribution for a tile, $p$ is the pedestal count, and $s$ is the peak count corresponding to one photoelectron referred to as the single photoelectron peak (SPP) in what follows.

A total of 1500 k cosmic-ray events were collected to obtain pulse-height distributions for tiles, which took about 1.5 days. We selected events in

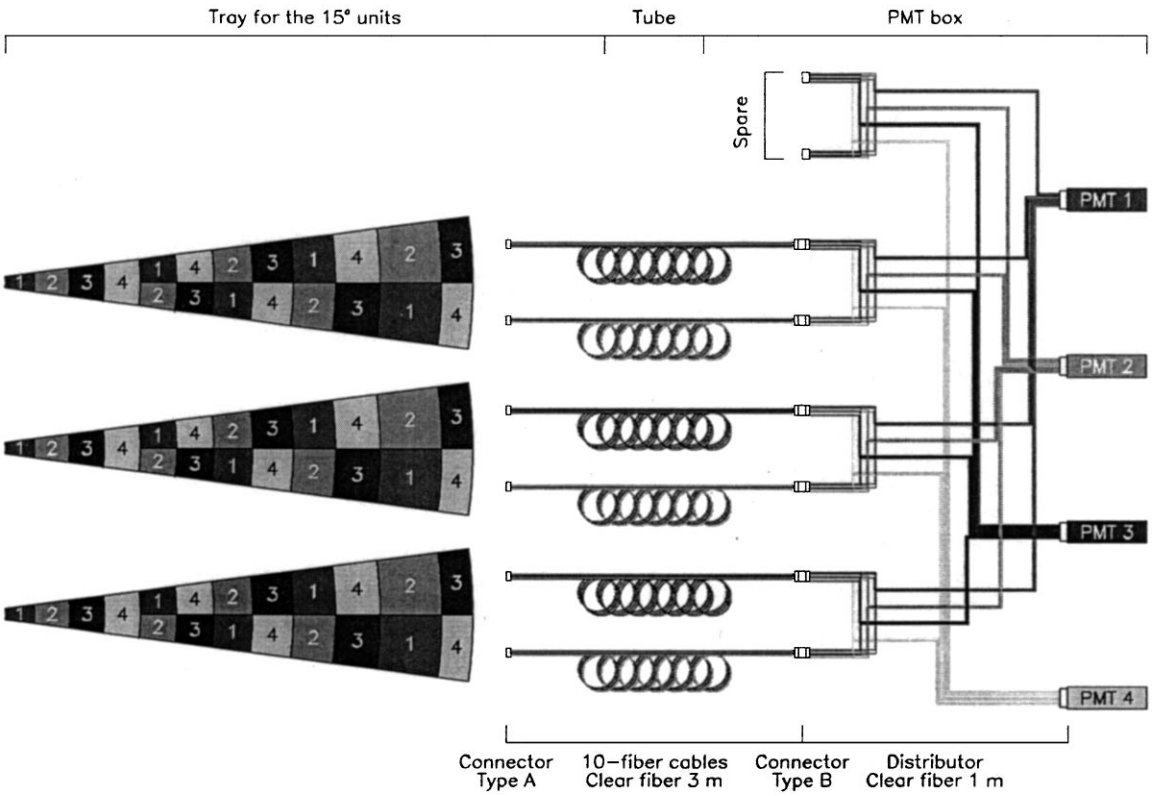


Fig. 3. Optical readout-system for three 15° units in the cosmic-ray test setup.

which only one track was reconstructed and the hit position was in a fiducial region of the tile (a few centimeters away from tile edges depending on the tile size). Statistical uncertainties were 1–2% for most of the tiles.

We measured the pedestal and the SPP count for each of the 20 readout PMTs by using a tile–fiber sample exposed to a β-ray source ($^{90}$Sr). The light yield of the tile–fiber sample was controlled to be small enough so that one-photoelectron events were dominant except pedestal events. The measurement was done every time after completing cosmic-ray data taking. The pedestal count was calculated as the average count in the $\pm 2$ bins around the highest peak bin. The SPP count was obtained by fitting the pulse-height distribution to a Gaussian function in a relevant region. The typical pedestal and SPP count were 80 and 40, respectively. Instability of the pedestal count was smaller than 1 count. Reproducibility of the SPP measurement was $\pm 2\%$ by peak and the RMS was smaller than 1%.

A demonstration of the light yield measurement is given in Fig. 4. One can note that there are some pedestal events in the pulse height distribution, while the expected pedestal fraction for this example (7.3 pe) is negligible. The contribution of this misrecontruction of events is found to be a few percent level for most of the tiles, which is not a problem for the quality control.

Systematic uncertainty of the light yield measurement was estimated by checking the reproducibility. It was found to be 1.8% for a short term and 4.0% for the entire quality control process (about 1.5 years).

There are 300 optical channels in our system whose responses are basically different due to differences of the light transmission at the connectors,

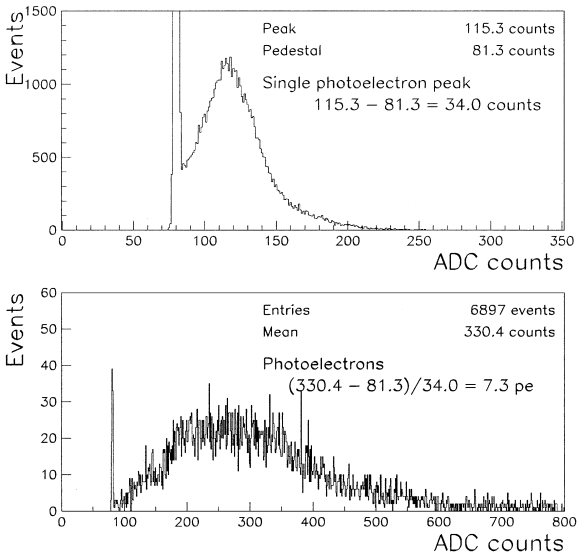


Fig. 4. Example of the light yield measurement.

the attenuation length of the fibers, and the quantum efficiency of the PMTs. In order to make meaningful comparisons of the light yield between different 15° units and to estimate light yield variation along longitudinal layers of tower, the readout channels were calibrated by using calibrated light sources. The RMS of the response of the readout channels was $\simeq 10\%$. Uncertainty of the calibration was estimated to be 2.4% which was dominated by non-uniformity of the optical connectors.[2]

## 4. Quality control

The quality control process for individual 15° unit started from a visual inspection which included checks of the optical connector surface by using a CCD camera. One of the problems at this stage that we experienced was loose fiber attachment to the connector resulting in fiber slippage with respect to the connector edge. The units which passed the visual inspection were tested with the cosmic-ray test stand. The quality control criteria were that

- the light yield of a tile must be larger than 3 and 10 pe for the EM and the preshower units, respectively;
- the light yield must be within $\pm 30\%$ from the corresponding tower average.[3]

Note that we required the light yield for the preshower twice as large as original requirement (5 pe/MIP) by taking into account of the higher quantum efficiency of the H1161GS used in the cosmic-ray test than that of the MAPMT by typically a factor of 2.

### 4.1. Results for EM units

Fig. 5 shows distributions of the number of photoelectrons. The average light yields as a function of tile number and layer number are given in Figs. 6(a) and (b), respectively. Note that the light yield of tile number 1 which is the smallest in a unit is typically smaller than 3 pe because of the geometrical limit on embedding the readout fiber to collect enough light.

We did not explicitly control the light yield variation for the tiles with the same size, but it is one of the quantities representing uniformity of the products. Fig. 7(a) shows the result. The light yield variation for the same size tiles is estimated to be 7.8% by subtracting an estimated measurement uncertainty of 3.4% in quadrature. The light yield variation along the longitudinal layers of tower is given in Fig. 7(b). We estimate the light yield variation to be 9.5% by subtracting an estimated measurement uncertainty of 4.9% in quadrature. We let a small fraction of units which were outside the $\pm 30\%$ limit pass our control, since they had little effect on the overall quality.

We note that the longitudinal light-yield variation in tower obtained from the cosmic-ray data does not include non-uniformity of actual readout system between the 15° units and the PMTs,

[2] Note that the connectors of the calibration light source and those of the 15° units are different.

[3] The *tower average* for the preshower unit is the average over tiles with the same size.

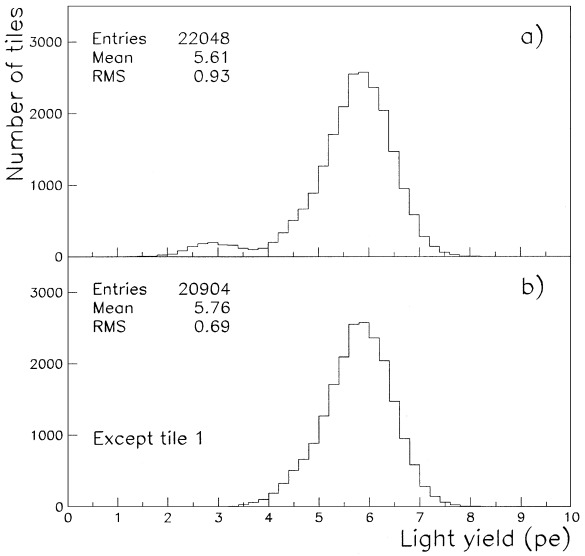


Fig. 5. Light yield distribution for (a) all the tiles and (b) the tiles except tile number 1.

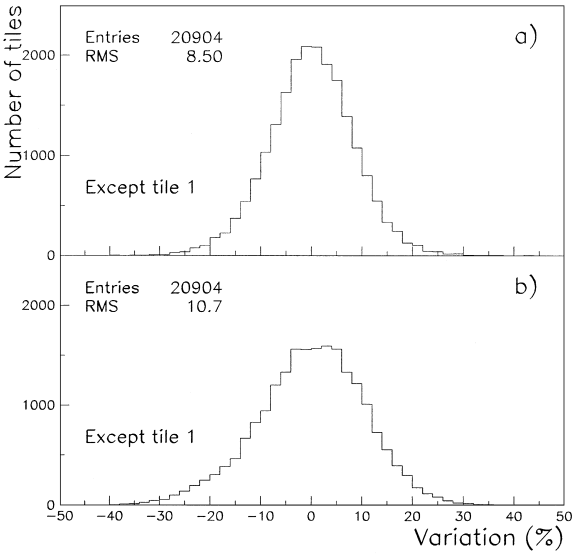


Fig. 7. Light yield variation (a) for the same-size tiles and (b) along the longitudinal layers of tower.

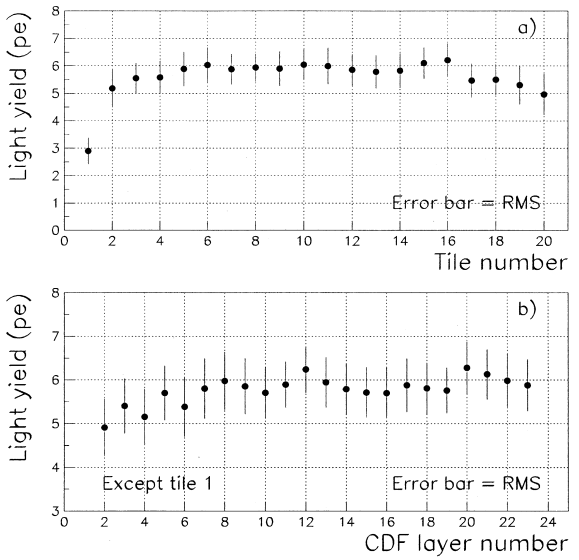


Fig. 6. Average light yield (a) as a function of tile number and (b) as a function of layer number. The error bar represents RMS.

because we used the same fiber cables all the time in the cosmic-ray tests. In real operation, light outputs from the units of each layer are readout by different fiber cables, then the unit-based arrangement is converted to the tower-based one, and finally they are lead to a single PMT. The non-uniformity from this part is expected to be a few percent which will not be a problem.

We evaluate the light leakage by $(\sum_i N_i)/N_{\text{seed}} \times 100\%$, where $N_{\text{seed}}$ is the light yield of a tile with cosmic-ray hits (seed tile), $N_i$ is the light yield of tile $i$, and the sum is over all the tiles adjacent to the seed tile in a unit. We used one PMT to measure the light yield of the seed tile and three PMTs to calculate the sum of the light yield of the adjacent tiles. The results are shown in Fig. 8. The distribution of all the tiles except tile number 1 has a peak around 0.15% and a symmetric shape with an RMS variation of 0.76%. The light leakage was at the most 4%. The pedestal fluctuation of the PMTs is about 1 ADC count in RMS which corresponds to about 0.025 pe. Therefore, the pedestal fluctuation of the sum of the three PMTs is estimated to be around 1.7 ADC counts (0.043 pe) which corresponds to an RMS variation of about $\simeq 0.75\%$ in terms of the light leakage. The dashed curve shown in the figure is the distribution expected for the pedestral fluctuation. It describes the measured distribution well and no significant light leakage was observed.

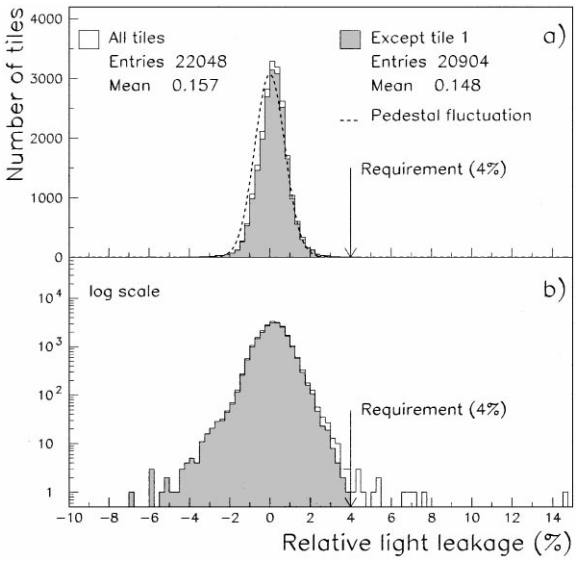


Fig. 8. Distribution of the light leakage in (a) the linear scale and (b) the logarithmic scale. The dashed line is the distribution expected for the pedestal fluctuation.

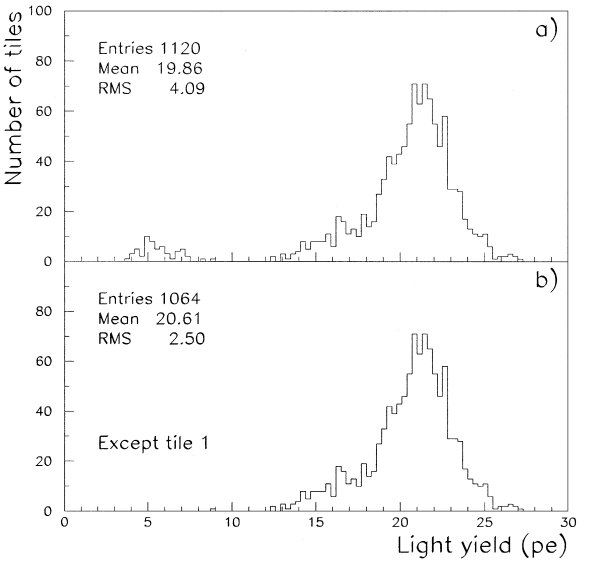


Fig. 9. Light yield distribution for the preshower units; (a) all the tiles and (b) the tiles except tile number 1.

### 4.2. Results for preshower units

Fig. 9 shows distributions of the light yield. Except the number 1 tiles, only one tile gave a low response out of the specification, and that unit was rejected. We also calculated the average light yield for each tile number as shown in Fig. 10.

The light yield variation for the same-size tiles is shown in Fig. 11. Subtracting an estimated measurement uncertainty of 3.4% in quadrature, we estimate the light yield variation to be 7.9%.

Fig. 12 shows distributions of the light leakage. The distribution of all the tiles except tile number 1 has a peak around 2.2% and an RMS variation of 1.3%. The light leakage was at the most 7.4%. The dashed curve shown in the figure is the distribution expected for the pedestal fluctuation. The measured light leakage is significantly larger than the pedestal fluctuation, but still within the specification.

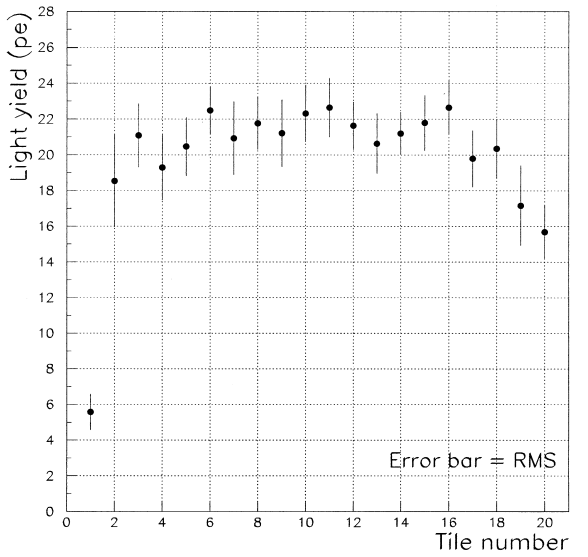


Fig. 10. Average light yield for the preshower units as a function of tile number. The error bar represents RMS.

## 5. Performance simulation

Using the GEANT Monte Carlo program, we simulated calorimeter responses for electrons with energies of 10, 100, and 200 GeV to estimate the non-linearity and the energy resolution of the calorimeter. In this simulation, we used the measured responses of the 15° units obtained from the cosmic-ray tests.

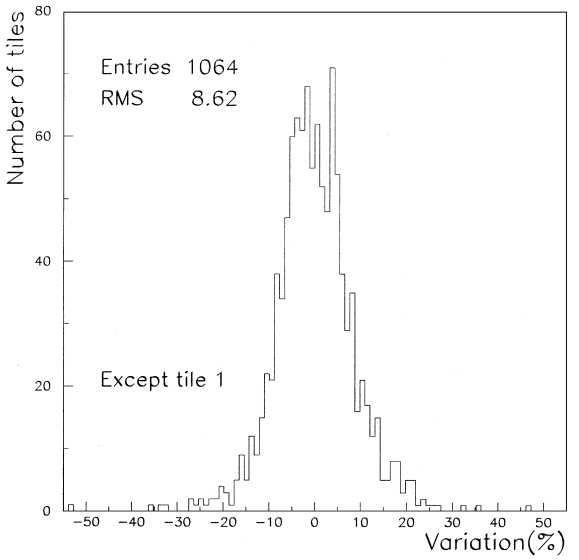


Fig. 11. Light yield variation for the same-size tiles of the preshower units.

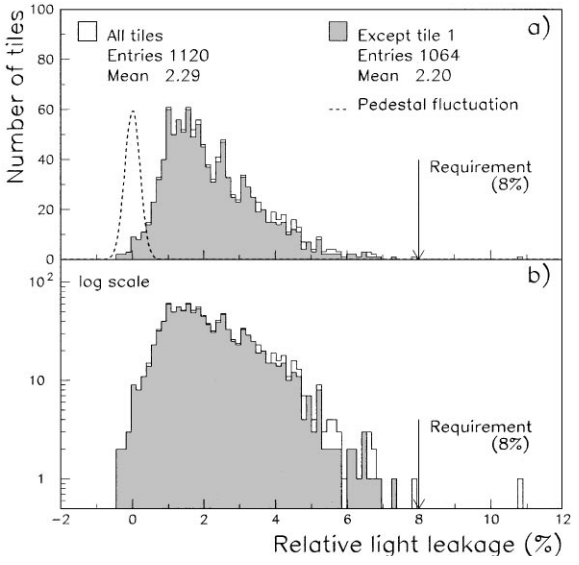


Fig. 12. Distribution of the light leakage for the preshower tiles in (a) the linear scale and (b) the logarithmic scale. The dashed line shows the distribution expected for the pedestal fluctuation.

### 5.1. GEANT simulation data

As shown in Fig. 13, we used a material configuration similar to the real calorimeter [1,2]. There

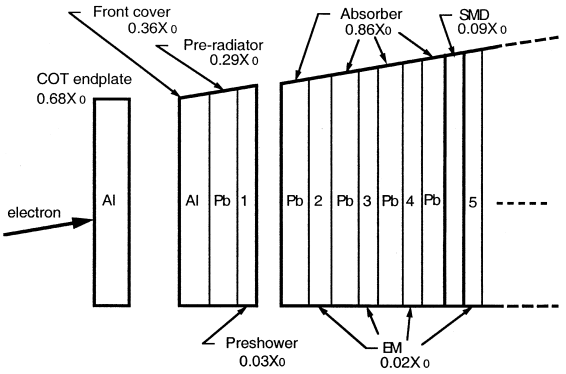


Fig. 13. Materials for the GEANT EM shower simulation.

were 23 sampling layers, where the first preshower layer consisted of a lead plate of $0.29X_0$ and a preshower unit of $0.03X_0$, and the rest of the layers were lead of $0.86X_0$ and EM units of $0.02X_0$. Both the preshower and the EM units included top (1.7 mm) and bottom (0.8 mm) plastic cover plates. A shower maximum detector (SMD) consisting of plastic scintillator stripes occupies just before the EM unit at layer 5 where we inserted a scintillator plate of $0.09X_0$ accordingly. We put aluminum of $0.36X_0$ as the front calorimeter cover and also aluminum of $0.68X_0$ to simulate the end plate of the central tracking detector (COT).

Electrons were injected into the center to each tower along 10 different polar angles ($\theta$) according to the tower geometry (tower 3 and even numbered towers). Here tower 1 and 20 were not considered because of too low light yield and incomplete tower geometry in depth, respectively. The simulated data of energy deposition were commonly used to calculate calorimeter responses at different azimuthal angles in conjunction with the measured responses of the 15° units.

### 5.2. Non-linearity and preshower weight

We calculate the total energy deposition as a weighted sum of energies in the preshower detector and the EM calorimeter

$$E_{\mathrm{dep}}^{\mathrm{tot}} = W \times E_{\mathrm{dep}}^{\mathrm{PR}} + E_{\mathrm{dep}}^{\mathrm{EM}}$$

and consider how the preshower weight affects the calorimeter non-linearity. Here we define $E_{\rm dep}^{\rm PR}$ and $E_{\rm dep}^{\rm EM}$ by

$$E_{\rm dep}^{\rm PR} = \sum_{t}^{\rm cluster} E_{\rm dep}(t, l=1),$$

$$E_{\rm dep}^{\rm EM} = \sum_{t}^{\rm cluster} \left( \sum_{l=2}^{23} E_{\rm dep}(t,l) \right),$$

where $E_{\rm dep}(t,l)$ is the energy deposited in the $t$th tile at the $l$th layer and cluster means the range for tower summation (clustering) around the central tower hit by electrons (seed tower). We compare four types of clustering: the "ideal" case, $5\times5$, $3\times3$, and $1\times1$, where the ideal case is obtained from another set of simulation data in which each of the materials is expanded to a single large piece with a size of 8.4 m × 8.4 m. For each of the four different clustering cases, the averages of $E_{\rm dep}^{\rm PR}$, $E_{\rm dep}^{\rm EM}$ and $E_{\rm dep}^{\rm tot}$ (with $W=1$) as a function of seed-tower number are shown in Figs. 14 and 15 for 10 and 100 GeV electrons, respectively. The preshower energy increases with the tower number because the effective radiator thickness increases according to $1/\cos\theta$. The $5\times5$ and $3\times3$ clustering cases for the preshower are consistent with the ideal case, while the $1\times1$ clustering is missing by about 5% (10%) of the deposited energy for 10 (100) GeV electrons. For the EM energy, the $3\times3$ clustering is missing 2% at most. The decrease of the energy deposition in the calorimeter along with the tower number is due to the decrease of effective sampling rate by the same $1/\cos\theta$ effect as for the preshower energy. We see a strong dependence on the tile size in the $1\times1$ case especially around tower number 3 and 4. This effect still remains at 1% level even for the $3\times3$ and $5\times5$ cases particularly for 10 GeV electrons.

We evaluate the response non-linearity by comparing energy deposition by 100 GeV electrons with that by 10 or 200 GeV electrons. We define the response non-linearity at an energy of $E$ GeV, $\delta(E)$, as

$$\delta(E) = \left( \frac{\langle E_{\rm dep}^{\rm tot}(E)\rangle}{\langle E_{\rm dep}^{\rm tot}(100)\rangle} \times \frac{100}{E} - 1 \right) \times 100\%$$

where $\langle E_{\rm dep}^{\rm tot}(E)\rangle$ is the mean value obtained by fitting a Gaussian function to the distribution. We

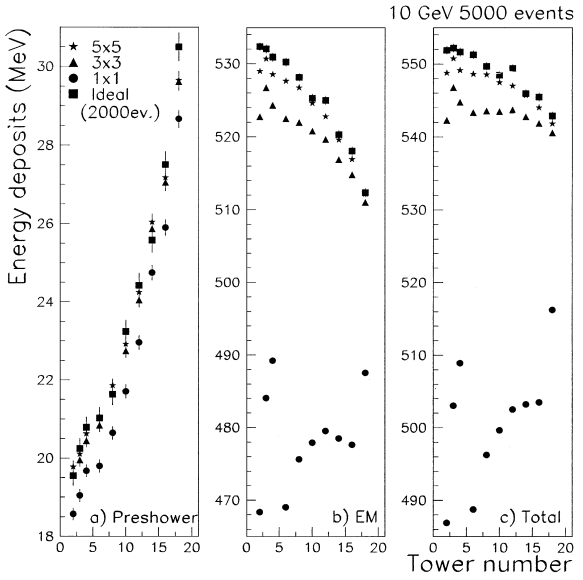


Fig. 14. Average energy deposition in (a) the preshower tiles ($E_{\rm dep}^{\rm PR}$), (b) the EM towers ($E_{\rm dep}^{\rm EM}$), and (c) the sum of them for 10 GeV electrons as a function of tower number. The number of events is 5000 for the $5\times5$, $3\times3$ and $1\times1$ clustering, and 2000 for the ideal case.

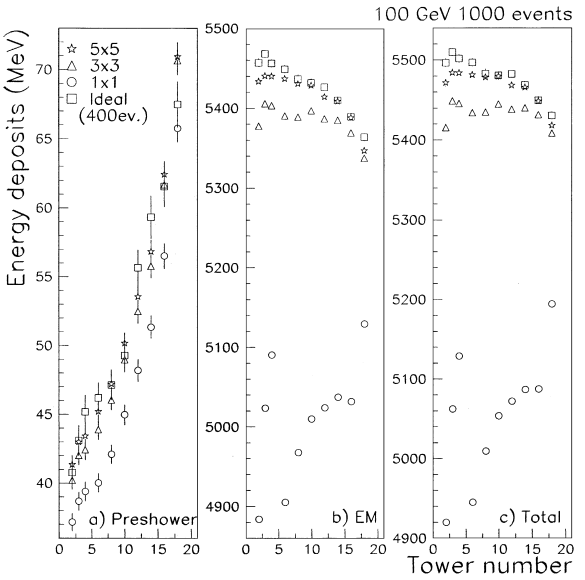


Fig. 15. Average energy deposition in (a) the preshower tiles ($E_{\rm dep}^{\rm PR}$), (b) the EM towers ($E_{\rm dep}^{\rm EM}$), and (c) the sum of them for 100 GeV electrons as a function of tower number. The number of events is 1000 for the $5\times5$, $3\times3$ and $1\times1$ clustering, and 400 for the ideal case.

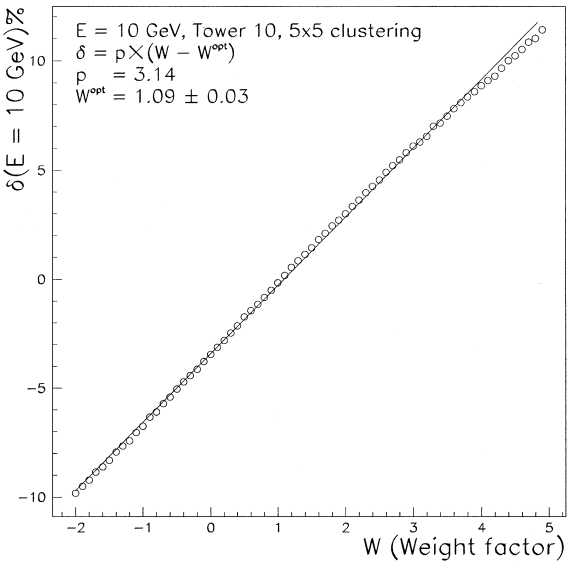


Fig. 16. Non-linearity versus preshower weight factor at tower 10 for the electron energy of 10 GeV by using the $5 \times 5$ clustering. The solid line shows the fitted linear function.

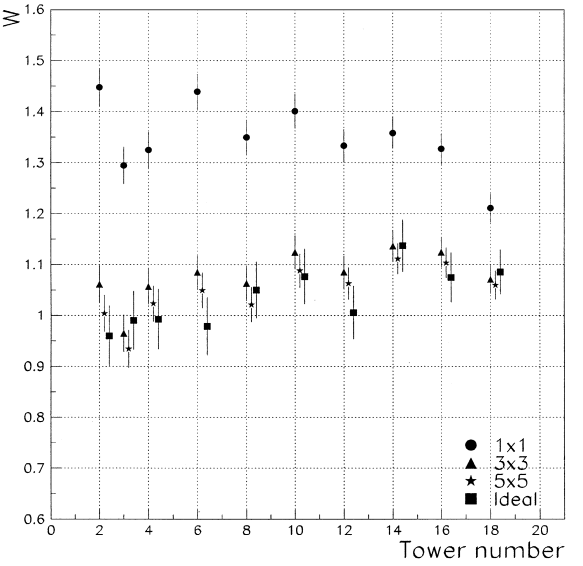


Fig. 17. Optimum preshower weight factor as a function of tower number.

minimize the non-linearity by varying the weight of the preshower energy. Fig. 16 shows the non-linearity at tower 10 for 10 GeV electrons as a function of weight factor obtained by using the $5 \times 5$ clustering. We see that the non-linearity is over $-3\%$ if we do not add the preshower energy to the EM energy ($W = 0$). From a linear fit, we obtain the optimum weight factor as $W^{\text{opt}} = 1.09 \pm 0.03$ at $\delta = 0$. The uncertainty of $W^{\text{opt}}$ is estimated by looking at changes of $W^{\text{opt}}$ when the linear fitting is repeated with shifting the data points simultaneously upward and downward by one standard deviation of individual statistical uncertainty.

Fig. 17 shows the optimum weight factor as a function of tower number for the four types of clustering. The optimum weight factors have little dependence on the tower number except for the $1 \times 1$ case. However, we can see small dips at tower number 3 for the $3 \times 3$ and $5 \times 5$ cases which are reflecting bumps at tower number 3 seen in Fig. 14.

### 5.3. Calorimeter response

Now we include the measured responses obtained from the cosmic-ray tests. We convert the deposited energy in each tile in each layer, $E_{\text{dep}}(t, l)$, to the number of photoelectrons, $N_{\text{pe}}(t, l)$, as follows:

$$N_{\text{pe}}(t, l) = \frac{E_{\text{dep}}(t, l)}{E_{\text{MIP}}(l)} \times N_{\text{pe}}^{\text{MIP}}(t, l)$$

where $E_{\text{MIP}}(l)$ is the average energy deposition per MIP per tile in the $l$th layer and $N_{\text{pe}}^{\text{MIP}}(t, l)$ is the number of photoelectrons per MIP per tile which was obtained from the cosmic-ray tests. The $E_{\text{MIP}}(l)$ is estimated by a Monte Carlo simulation for 10 GeV muons injected perpendicular to the calorimeter without absorber and obtained as $E_{\text{MIP}}(l = 1) = 1.784$ MeV/MIP for the preshower layer and $E_{\text{MIP}}(l \geq 2) = 0.699$ MeV/MIP for the EM layers. The preshower and the EM responses of tower $t$ are given by

$$N_{\text{pe}}^{\text{PR}}(t) = 0.5 \times N_{\text{pe}}(t, l = 1),$$

$$N_{\text{pe}}^{\text{EM}}(t) = \sum_{l=2}^{23} N_{\text{pe}}(t, l).$$

The factor 0.5 implies that the quantum efficiency of the MAPMT which will be used in the real operation for the preshower detector is half of the

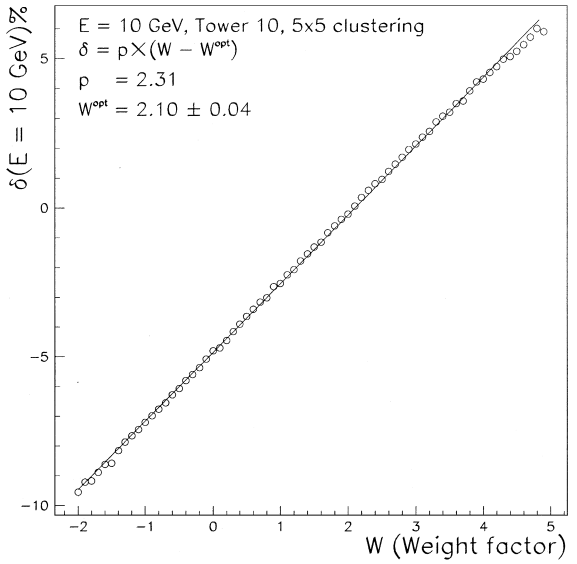


Fig. 18. Non-linearity versus preshower weight factor at tower 10 for the electron energy of 10 GeV by using the $5\times5$ clustering after taking into account of the light yield measured in the cosmic-ray tests. The solid line shows the fitted linear function.

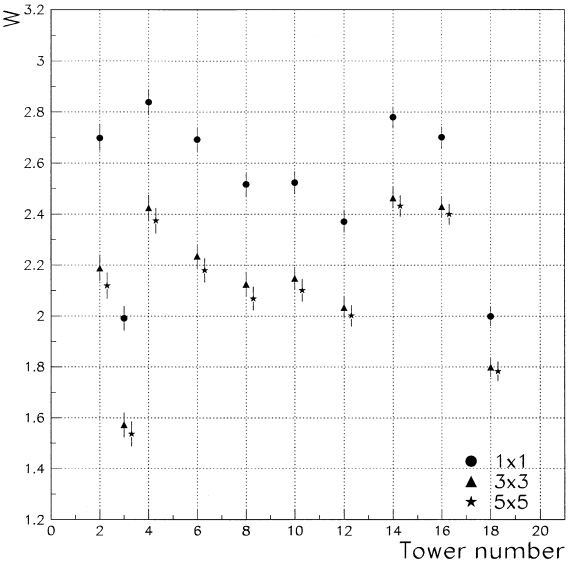


Fig. 19. Optimum preshower weight factor as a function of tower number after taking into account of the light yield measured in the cosmic-ray tests.

PMTs used in the cosmic-ray tests. We smear $N_{\mathrm{pe}}^{\mathrm{PR}}(t)$ and $N_{\mathrm{pe}}^{\mathrm{EM}}(t)$ according to Poisson distributions to take into account of the photostatistics. Finally the total calorimeter response is calculated by summing up tower responses around the seed tower

$$N_{\mathrm{pe}}^{\mathrm{tot}} = \sum_{t}^{\mathrm{cluster}} (W \times N_{\mathrm{pe}}^{\mathrm{PR}}(t) + N_{\mathrm{pe}}^{\mathrm{EM}}(t)).$$

Note that the preshower weight factor defined here is not the same as the one in the previous section.

We minimize the non-linearity by varying the weight of the preshower response as before. For simplicity, we set tile responses to the average value for the corresponding tile number of each layer. Fig. 18 shows the non-linearity at tower 10 for 10 GeV electrons as a function of weight factor obtained by using the $5\times5$ clustering. The optimum weight factor is obtained to be $2.10 \pm 0.04$. The difference from the preshower weight factor obtained in the previous section is due to the inserted factor of 0.5 in converting preshower energy to the number of photoelectrons and the layer-to-layer light yield variation which changes the relative weight of the preshower response. The results for various towers and comparison between the different clustering cases are summarized in Fig. 19.

We check the variation of the optimum weight factor when we take into account of the light yield variation. We repeat estimation of the optimum weight factor for tower 10 by fluctuating the average light yield according to a Gaussian distribution with the measured sigma. From 100 trials, the RMS is found to be 0.4 with the $5\times5$ clustering.

### 5.4. Simulated calorimeter performance

A number of possibilities exist in arranging the 15° units along the azimuthal direction to construct the calorimeter. In order to see if the calorimeter performance depends on the unit arrangement, we compare the following two different cases:

1. Random configuration – we randomly put the 15° units to construct the calorimeter. We made 100 sets of different configurations;

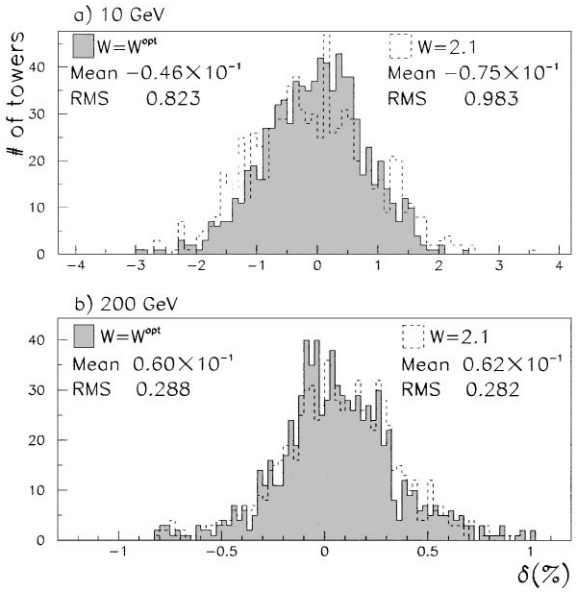


Fig. 20. Distribution of the non-linearity over towers except towers 1, 19, and 20 for the optimized configuration for (a) 10 GeV and (b) 200 GeV electrons. The dashed lines show the case that we fix the preshower weight factor to 2.1, while for the solid lines we use different optimum factors depending on the tower number.

2. Optimized configuration – in each layer, the 15° units are placed in the descending order of the average response of each unit. In this configuration, the response variations of the 15° unit in the azimuthal and the longitudinal directions tend to be smoother than the case of the random configuration.

We consider only the $5 \times 5$ clustering from now on.

We calculate the non-linearity at each tower for 10 and 200 GeV electrons using the optimized 15°-unit configuration. The resulting non-linearity distributions are shown in Fig. 20. In the figure, we compare the cases when we apply different optimum weight factors according to the tower number as given in Fig. 19[4] and the average of them (2.1)

[4] For the odd numbered tower not shown in the figure, we use the same weight factor as for the even numbered tower with the same polar angle.

Table 1
Comparison of the non-linearity between the optimized and the random configurations

| | $\delta$ at 10 GeV (%) | | $\delta$ at 200 GeV (%) | |
|---|---|---|---|---|
| | Mean | RMS | Mean | RMS |
| Optimized | −0.05 | 0.82 | 0.06 | 0.29 |
| Random | −0.05 | 0.95 | 0.06 | 0.31 |

commonly to all the towers. In any case, the RMS of the non-linearity distribution is $\simeq 1\%$ at most.

Using tower-dependent preshower weight factors, we compare the non-linearities between the two configurations in Table 1. For the random configuration, we calculate the average non-linearity and the RMS for each configuration out of 100 trails. The results shown in the table are the averages over the 100 different sets of configuration. We see no significant difference between the two unit-configurations.

We do a similar study for the energy resolution. Using the optimum preshower weight factors for the optimized 15°-unit configuration, the distribution of the energy resolution over towers is obtained as shown in Fig. 21. The average values are plotted as a function of energy in Fig. 22. By fitting to the form of $\sqrt{\sigma_s^2/E + \sigma_c^2}$, we obtain $\sigma_s = (16.5 \pm 0.75)\%$ and $\sigma_c = (0.61 \pm 0.26)\%$. The results including other choices of the configuration and the preshower weight factor are summarized in Table 2. We do not see any significant differences in all cases and the results are consistent with the required performance.

## 6. Conclusions

We performed cosmic-ray tests as a quality control of the CDF Plug Upgrade EM calorimeter and the CDF Plug preshower detector. Using HAMAMATSU R4125 as the photon readout, the average light yields were obtained to be 5.8 and 21 photoelectrons per MIP for the EM tile–fiber units and the preshower units, respectively. The light yield variation along the longitudinal layers of EM

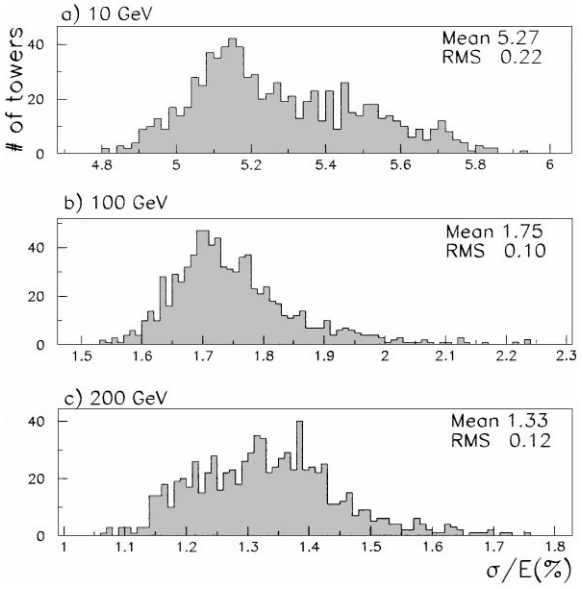


Fig. 21. Distribution of the energy resolution over towers except towers 1, 19, and 20 for (a) 10 GeV, (b) 100 GeV, and (c) 200 GeV electrons.

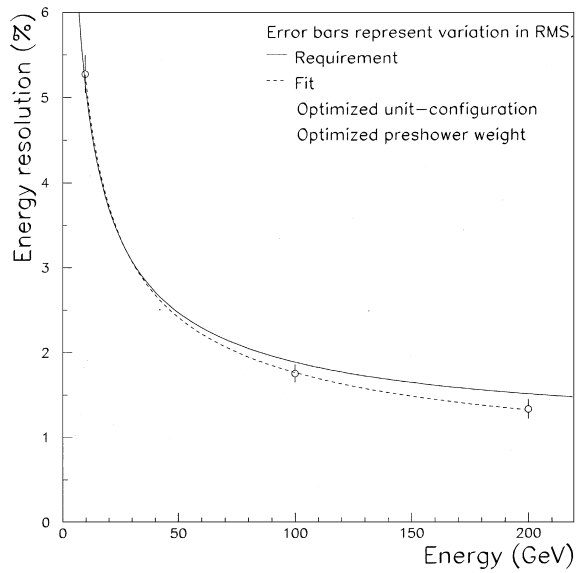


Fig. 22. Energy resolution averaged over towers except towers 1, 19, and 20 as a function of energy. The error bar represents RMS of the energy-resoultion distribution over towers. The solid curve shows the requirement.

Table 2
Estimated energy resolution

| Configuration | Weight factor | $\sigma_s$(%) | $\sigma_c$(%) |
|---|---|---|---|
| Optimized | Tower dependent | $16.5 \pm 0.75$ | $0.61 \pm 0.26$ |
| | Fixed to 2.1 | $16.5 \pm 0.67$ | $0.62 \pm 0.24$ |
| Random | Tower dependent | $16.6 \pm 0.74$ | $0.62 \pm 0.25$ |
| | Fixed to 2.1 | $16.6 \pm 0.70$ | $0.63 \pm 0.25$ |

tower after the quality control was found to be 10%. The light yield variation of the preshower tiles with the same size was found to be 8%. The calorimeter performance was studied by using a GEANT EM shower simulation in conjunction with the light-yield data obtained from the cosmic-ray tests. The linearity of the response was improved by adding preshower response to EM response. It was possible to achieve the non-linearity of 1% level for electrons in the energy range of 10–200 GeV by using a common preshower weight factor to all the towers. The stochastic term and the constant term of the energy resolution were estimated to be 16% and 0.7%, respectively. These results were consistent with the required performance. It was also found that the calorimeter performance did not depend on the details of the 15° units arrangement.

## References

[1] G. Apollinari, P. de Barbaro, M. Mishina, in: A. Menzione et al. (Eds.), Proceedings of the Fourth International Conference on Calorimetry in High Energy Physics, La Biodola, Italy, 1993, World Scientific, Singapore, 1994, p. 200.
[2] R. Blair et al., CDF Collaboration, CDF II Technical Design Report, FERMILAB-Pub-96/390-E, 1996, p. 9-1.
[3] T. Asakawa et al., Nucl. Instr. and Meth. A 340 (1994) 458.
[4] S. Aota et al., Nucl. Instr. and Meth. A 352 (1995) 557.
[5] S. Kim, CDF Collaboration, Nucl. Instr. and Meth. A 360 (1995) 206.
[6] S. Aota et al., Nucl. Instr. and Meth. A 420 (1999) 48.
[7] Y. Ikegami, Ph.D. thesis, University of Tsukuba, 1990, Report No. UTPP-35.
[8] S. Aota et al., Nucl. Instr. and Meth. A 357 (1995) 71.